Environmental Science
Processes & Impacts

PAPER

Cite this: *Environ. Sci.: Processes Impacts*, 2019, **21**, 1729

NO_2 and natural organic matter affect both soot aggregation behavior and sorption of *S*-metolachlor†

Gabriel Sigmund, *[ab] Stephanie Castan, [b] Christopher Wabnitz,[a] Rani Bakkour, [a] Thorsten Hüffer, [b] Thilo Hofmann [b] and Martin Elsner *[ac]

Received 24th July 2019
Accepted 23rd August 2019

DOI: 10.1039/c9em00354a

rsc.li/espi

Soot is an important carbonaceous nanoparticle (CNP) frequently found in natural environments. Its entry into surface waters can occur directly *via* surface runoff or infiltration, as well as *via* atmospheric deposition. Pristine soot is likely to rapidly undergo aggregation and subsequent sedimentation in aquatic environments. Further, soot can sorb a variety of organic contaminants, such as *S*-metolachlor (log K_D = 3.25 ± 0.12). During atmospheric transport, soot can be chemically transformed by reactive oxygen species including NO_2. The presence of natural organic matter (NOM) in surface waters can further affect the aquatic fate of soot. To better understand the processes driving the fate of soot and its interactions with contaminants, pristine and NO_2-transformed model soot suspensions were investigated in the presence and absence of NOM. NO_2-oxidized soot showed a smaller particle size, a higher number of particles remaining in suspension, and a decreased sorption of *S*-metolachlor (log K_D = 2.47 ± 0.40). In agreement with findings for other CNPs, soot stability against aggregation was increased for both pristine and NO_2 transformed soot in the presence of NOM.

Environmental significance

Soot is an important carbonaceous nanoparticle (CNP) frequently found in natural environments with abundances up to 10^4 times higher compared to widely studied engineered CNPs. Although soot CNPs are highly relevant to surface water systems, to date, the nano-particulate properties of soot in the natural environment have received only a little attention. Here we investigate the effects of atmospheric transformation with NO_2 on soot aggregation and contaminant sorption using the widely found herbicide *S*-metolachlor as a model contaminant. The findings of this study will help to better understand the colloidal behavior of pristine soot compared to atmospherically transformed soot and bring forward hitherto underexplored aspects of soot as a naturally occurring CNP.

1. Introduction

Due to climate change and shifting land usage, wildfires have increased in abundance and intensity in recent years and are expected to further increase in the future.[1] Wildfires and incomplete combustion of biomass and fossil fuel can form a considerable amount of carbon nanoparticles (CNPs). One type of CNP is soot, the finest fraction of incomplete combustion residues formed *via* re-condensation and nucleation of organic compounds from the gas phase during the combustion process.[2] Annual production of soot transportable *via* the atmosphere is estimated to be 17 Tg per year.[3] Thus, soot emissions are expected to be at least 10^4 times more abundant compared to widely studied engineered CNPs including graphene oxides, fullerenes and carbon nanotubes.[4]

Once released into the atmosphere, soot can undergo chemical transformation, resulting in changes in the surface chemistry. Key processes for atmospheric soot transformation are photochemical redox reactions with NO_x, SO_x, O_3 and other reactive oxygen species in the atmosphere.[5,6] Over time NO is predominantly oxidized to NO_2 in the atmosphere, thereby making NO_2 the most abundant NO_x reactive oxygen species in the atmosphere. The reaction of NO_2 with soot was previously elucidated using spectroscopic techniques where infrared bands were attributed to acidic functional groups (C(=O)O–R, R–NO_2, and R–ONO are the main functionalities).[7,8]

Soot – pristine or atmospherically transformed – can reach water bodies directly *via* atmospheric deposition and indirectly *via* surface runoff and infiltration. In suspension, soot can remain colloidally stable, *i.e.* dispersed, and be transported in the aqueous phase, or it can aggregate and deposit. The

[a]*Chair of Analytical Chemistry and Water Chemistry, Technical University of Munich, Marchioninistrasse 17, 81377 Munich, Germany. E-mail: m.elsner@tum.de*

[b]*Department of Environmental Geosciences, Centre for Microbiology and Environmental Systems Science, University of Vienna, Althanstraße, 1090 Wien, Austria. E-mail: gabriel.sigmund@univie.ac.at*

[c]*Institute of Groundwater Ecology, Helmholtz Zentrum München, Ingolstädter Landstrasse 1, 85764 Neuherberg, Germany*

† Electronic supplementary information (ESI) available. See DOI: 10.1039/c9em00354a

aggregation behavior of soot is expected to depend mainly on the soot surface charge, the presence of natural organic matter (NOM), and the ionic composition of the aqueous environment.[4] A recent study by Chen *et al.*[9] found that soot aggregation followed classic Derjaguin–Landau–Verwey–Overbeek (DLVO) theory,[10–12] describing the aggregation behavior of particles as a combination of van der Waals attraction and electrostatic repulsion. Depending on the aqueous chemistry, soot particles can remain stable against homo-aggregation in typical freshwater environments but are likely to aggregate under saline conditions (*e.g.* estuaries) due to the compression of the electrical double layer at higher ionic strengths. The effect of chemical transformation (*e.g.* with NO_2) on the aggregate size of soot particles has to date received little attention. But with an increasing negative surface charge and the presence of NOM soot particles are expected to form increasingly stable suspensions.[4]

In the water phase, soot has a strong adsorption affinity for a range of organic contaminants,[13–16] and because of its higher abundance compared to other CNPs, soot may significantly alter the fate of organic contaminants occurring in surface waters. From other CNPs it is known that the presence of NOM strongly affects particle aggregation and size and may also influence the sorption of organic contaminants due to changes in accessibility of sorption sites. For instance, a number of studies have shown that the presence of NOM can decrease the sorption affinity of carbon nanotubes for organic contaminants by competing for sorption sites and blocking the accessibility to micropores.[17–19] In contrast, both Wang *et al.*[20] and Hou *et al.*[21] found that NOM can increase the sorption affinity of organic contaminants to fullerene (nC_{60}) aggregates. This can be explained by an increase in accessible sorption sites due to decreased aggregation of nC_{60}. However, it remains unclear if similar effects occur with soot particle suspensions.

Pesticides are of environmental interest due to their widespread use and subsequent occurrence in natural waters. The herbicide *S*-metolachlor was selected as a model contaminant because of its (i) structural similarities to several other mobile organic contaminants, *i.e.* an aromatic ring substituted with polar functional groups, (ii) widespread use since 1978 in the USA and most European countries in corn and cotton production, and (iii) ecotoxicity in several aquatic species and birds.[22,23]

Sorption of organic compounds to "soot in water" is generally weaker than that to "soot in air", indicating that surface coverage with water suppresses the sorption by soot.[24] Thus, soot is expected to interact most strongly with organic contaminants when it is not fully wetted. Investigations into the pre-wetting kinetics of 1,2,4-trichlorobenzene and phenanthrene sorption by Nguyen *et al.*[14] showed that the complete wetting of soot requires more than 20 days and the corresponding degree of water coverage of soot affects sorption of organic contaminants. In addition, most soot particles are expected to be in suspension directly after their introduction into water bodies, before they can sediment. Therefore, with the intent to simulate environmentally meaningful scenarios, this study tackled the behavior of soot freshly introduced into water.

With the aim to obtain a better understanding of soot aggregation and interactions with organic contaminants, pristine and NO_2-transformed model soot was investigated in the presence and absence of NOM. We hypothesize that (i) NO_2-transformation and interactions with NOM increase the aggregation stability of soot and (ii) sorption of the model contaminant *S*-metolachlor is affected by changes in soot surface chemistry and interactions with NOM.

2. Materials and methods

Analytical grade *S*-metolachlor, methanol, acetonitrile, HNO_3, and $CaCl_2$ were purchased from Sigma-Aldrich (Germany). Suwannee River NOM was purchased from the International Humic Substances Society (USA). Milli-Q water was obtained using a Millipore instrument (Elix 5 Milli-Q Gradient A10, USA).

2.1 Soot preparation

Printex U soot was purchased from Evonik Carbon Black GmbH (Germany). Printex U is industrial soot with similarities to diesel engine soot which has previously been well characterized and used as a model soot sample.[26,27] To approximate transformation by NO_2, the soot was treated according to a protocol adapted from Wei *et al.*[28] In short, a thin layer of soot (approximately 2 mm) was exposed to saturated HNO_3 vapor containing NO_2 within a sealed glass desiccator under vacuum for 24 h at room temperature (25 °C) at a pressure of 200 mbar. The experimental setup did not allow for the measurement of NO_2 and other radical species that could also have formed (*i.e.* $OH^{\bullet}$). However, the degree of transformation was likely above the short term soot transformation expected in the atmosphere. Both pristine and NO_2-transformed soot were thereafter individually rinsed with Milli-Q water (250 mL g^{-1}, Fisher Scientific Phase Separating Filter Paper, Germany). Dry powdered soot samples were weighed into the respective background solution and vortexed for 30 s prior to any experiment.

2.2 Soot characterization

Sorbent suspensions of pristine and transformed soot were prepared in 1 mM $CaCl_2$ with or without NOM (10 mg L^{-1} DOC) and shaken for 24 h to obtain similar conditions to those in the sorption batch experiment (see Section 2.3). For selected samples DOC concentrations were measured after 24 h of shaking to determine the DOC loading on soot in the experiments (centrifugation at 1000*g* for 30 min and filtration, <0.22 μm, Shimadzu L series TOC). The hydrodynamic diameter of the particles was calculated by dynamic light scattering (DLS) with a ZetaSizer Nano ZS (Malvern Instruments Ltd., UK) with a laser of 632.8 nm wavelength at a fixed angle of 173°. Soot suspensions were vortexed for 10 s after the soot was transferred into the respective background solution. Including sample transfer and automatic adjustment of measurement settings by the instrument, the first measurement point was obtained after 80 s. Data for individual measurements of 10 s each for 30 min and for 1 min after 24 h of shaking were collected automatically. The autocorrelation function was fitted using the cumulant method, assuming a refractive index of 2.4. The polydispersity index (PdI) ranged from 0.2 to 0.8. Thereafter, the

electrophoretic mobility of the particles remaining in suspension after a settling period of 1 min was measured and converted to the ζ potential using 3 measurements with 20 runs each applying Henry's equation. The electrical conductivity was above 200 μS cm^{-1}. All samples were run in duplicate. The ash content was determined by weighing samples before and after heating at 750 °C for 6 h. The total C, H, and N contents were determined using an elemental analyzer (Elementar Vario Macro, Germany), and the O content was calculated by mass balance: O% = 100 − (C + H + N + ash). The BET specific surface area and pore size distribution were determined using N_2 physisorption following protocols previously described in Sigmund *et al.*[29] For scanning electron microscopy (Zeiss Sigma VP 300, acceleration voltage of 5 kV, working distance 3.6 mm, magnification 1.56k), single drops (20 μL) of the four soot suspensions after shaking for 24 h and settling for 1 min were placed on aluminum foil and dried in a desiccator. Fourier transform infrared spectra of dried samples (FTIR Bruker Tensor 27) were measured with a resolution of 4 cm^{-1} and 128 scans.

2.3 Sorption experiments

Sorption experiments were conducted at room temperature using the batch method based on OECD guideline 106 at 1 mM $CaCl_2$ and at eight different *S*-metolachlor concentrations in the range of 1 to 50 mg L^{-1} (remaining at least one order of magnitude below solubility).[30] Experiments for sorption of *S*-metolachlor and soot aggregation were carried out in suspensions comprising 10 mL aqueous phase loaded with 10 mg soot (*i.e.* 1 g soot per L), which is likely above most concentrations that may occur in the natural environment. The pH ranged between 6.8 and 7.4 throughout all experiments and did not significantly differ between pristine and NO_2-transformed soot. *S*-Metolachlor is a polar but non-ionizable compound and pH is thus not expected to strongly affect sorption even though functional groups on the soot surface may have been partially dissociated. The samples were spiked with *S*-metolachlor using a methanolic stock solution (volume < 1% to avoid co-solvent effects) and equilibrated on a shaker at 125 rpm for 24 h to reach equilibrium (pre-experiments showed that equilibrium was reached after 16 h; see Fig. S1 in the ESI†). Thereafter, a small volume of the suspension was filtered (<0.20 μm) and analyzed by HPLC (Phenomenex Luna C18 50 × 2.00 mm 5 μm column, detection at 210 nm with a Shimadzu DAD SPD-M20A detector). For the mobile phase a solvent mixture of Milli-Q water and acetonitrile was used (20/80 by volume). The limit of quantification for *S*-metolachlor was calculated to be tenfold the background noise and was 0.10 mg L^{-1}. Measured concentrations ranged between 0.4 and 40 mg L^{-1} and recoveries were calculated based on control samples without soot and used for concentration correction (recoveries ranged from 90 to 115% over the concentration range investigated). Sorbent loading was calculated *via* mass balance and fractions of *S*-metolachlor sorbed ranged from 6.5 to 85%.

2.4 Data analysis

Sorption isotherms were fitted with the Freundlich model:

$$q = K_F \times C_{aq}{}^n \quad (1)$$

where q (mg kg^{-1}) is the sorbent loading, C_{aq} (mg L^{-1}) is the aqueous concentration of the sorbate, K_F is the Freundlich coefficient, and n is the Freundlich exponent representing isotherm non-linearity (non-linearity increases as n deviates from unity). For a comparison among the soot suspensions and a prediction model, individual sorption coefficients (K_D, L kg^{-1}) were calculated with the Freundlich equation at a fixed aqueous concentration of 10 mg L^{-1}. Standard deviations (σ) of the Freundlich fit based K_D values at a given aqueous concentration were calculated using the uncertainty propagation equation.[2]

$$\sigma_q = \sqrt{\left(C_{aq}{}^n \sigma_{K_F}\right)^2 + \left(K_F C_{aq}{}^n \ln(C_{aq}) \sigma_n\right)^2} \quad (2)$$

Standard deviations for ppLFER-based K_D values at a given aqueous concentration were calculated using linear uncertainty propagation.

3. Results and discussion

3.1 Particle size decreased after transformation with NO_2 and interaction with NOM

The measured ζ-potential increased upon transformation from −8.5 ± 0.8 mV for pristine soot to −19.4 ± 0.4 mV for transformed soot (see Fig. 1), indicating the formation of negatively charged functional groups on the NO_2-transformed soot surface (*e.g.* R–C=O and/or R–COOH as indicated in FTIR spectra; see Fig. S2 in the ESI†). The formation of nitrogen- and oxygen-containing surface functional groups (C(=O)O–R, R–NO_2, and R–ONO) has previously been reported in the literature[7,8] and is additionally confirmed by an increase in the nitrogen and oxygen content (Table 2).

The increase in negative surface charge induced a decrease in size of the suspended soot particles based on DLS measurements (Fig. 1A). The measurements presented were obtained after 24 h of shaking to be comparable with sorption batch experiments. In addition, aggregation kinetics for the first 30 min after introduction of the soot into the water phase were determined (Fig. S3†).

The exposure of soot to NOM did not significantly change the elemental composition of the material ($p > 0.05$). This is consistent with the measured DOC loading of soot (17.7 ± 0.3 mg DOC per g soot). However, it increased the negative ζ-potential of soot to a similar degree as the NO_2 transformation, stabilizing the soot particles electrostatically against aggregation and decreasing their particle size (Fig. 1A). In contrast to the effect on pristine soot, NOM could not increase the negative surface charge of NO_2-transformed soot.

The number of particles remaining in suspension increased both after NO_2 transformation and after interaction with NOM (Fig. 1B), with the particle number concentration increasing up to 30-fold compared to pristine soot. The aggregate size decreased and the number of particles remaining in suspension was higher for NO_2-transformed soot with NOM compared to NO_2-transformed soot without NOM. This indicates that in

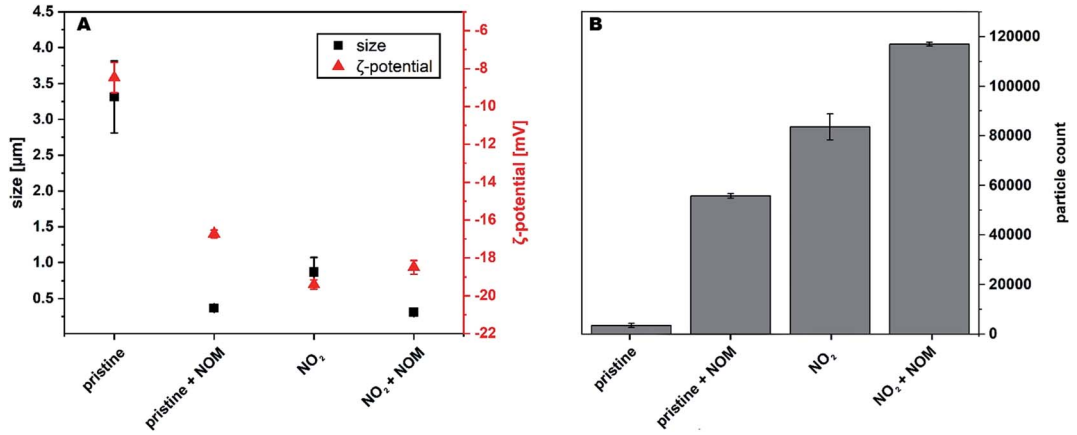

Fig. 1 (A) Particle size and ζ-potential of pristine soot decreased after NO_2-transformation and/or interaction with NOM. (B) Particle count increased with NO_2 transformation and in the presence of NOM.

Table 1 Selected properties of *S*-metolachlor. K_{OW} is the octanol water partition constant, *V* is the McGowan volume [m^3/100 mol], *E* is the excess molar refractivity, and *A* and *B* are the hydrogen bond acidity and basicity, respectively. The Abraham solute parameters *V*, *E*, *A* and *B* were obtained from the UFZ-LSER database[25]

Parameter	Value	Structure
log K_{OW}	3.13 (ref. 23)	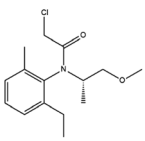
V	2.28 (ref. 25)	
E	1.11 (ref. 25)	
A	0.00 (ref. 25)	
B	1.25 (ref. 25)	

addition to electrostatic repulsion, steric effects might also play a role in the aggregation of soot in the presence of NOM.[4]

In good agreement with DLS measurements and particle mass remaining in suspension, scanning electron microscopy images confirmed the higher number and smaller size of suspended particles for NO_2 transformed soot compared to pristine soot. The stabilizing effect of NOM on soot aggregation could also be observed when comparing suspensions with and without NOM (Fig. 2), where differences in particle aggregation were more pronounced for pristine soot than for NO_2-transformed soot. It should be noted that relatively high soot concentrations were used in this study, and in many scenarios hetero-aggregation with other suspended particles in the natural environment is expected to outweigh the importance of the homo-aggregation investigated here.[4,31,32] However, the investigation of hetero-aggregation was not in the scope of this study and may be an interesting subject of further investigations building on the results presented here.

3.2 Sorption of *S*-metolachlor decreased upon NO_2-transformation and was not affected by the presence of NOM

Sorption (K_D) of *S*-metolachlor decreased by more than one order of magnitude after NO_2-transformation of soot and was not significantly affected ($p > 0.05$) by the presence of NOM (see Fig. 3 and Table 3). The decrease in sorption of *S*-metolachlor upon NO_2-transformation can be explained by a lower hydrophobicity of the soot surface and a less favorable accessibility of surface sorption sites.[4,33] Therefore, the higher number of O-containing surface functional groups on the NO_2-transformed soot is energetically favorable for H-bond interactions with water molecules, which increases the competitiveness of water molecules for sorption sites.[34,35] A decrease of organic contaminant sorption with an increase of O-functional groups is in good agreement with the literature findings on other carbonaceous materials, including carbon nanotubes,[36,37] fullerenes,[33,37] and biochars.[38,39]

The change in particle size was not reflected in the change in sorption of *S*-metolachlor. For instance, the particle size decreased for pristine soot after interaction with NOM, but did not significantly change the sorption. The BET specific surface area was 84.7 ± 3.1 and 89.9 ± 4.0 $m^2\ g^{-1}$ for pristine and NO_2 treated soot, respectively. Thus, the total specific surface area, which did not differ significantly between the materials, was not a limiting factor for *S*-metolachlor sorption under the conditions investigated. Also, under the conditions investigated, the presence of NOM did not suppress sorption due to competition for sorption sites, possibly because the high specific surface area offered enough sorption sites for both sorbates. This is consistent with previous observations on pyrene sorption to carbon nanotubes, which was only substantially suppressed by

Table 2 Elemental composition of soot particles upon transformation with NO_2

	C [%]	H [%]	N [%]	O [%]	Ash [%]
Pristine	93.76 ± 0.11	0.04 ± 0.09	0.47 ± 0.08	0.69 ± 0.56	5.12 ± 0.31
NO_2	84.91 ± 0.11	0.07 ± 0.09	1.19 ± 0.08	9.36 ± 1.26	2.74 ± 1.01

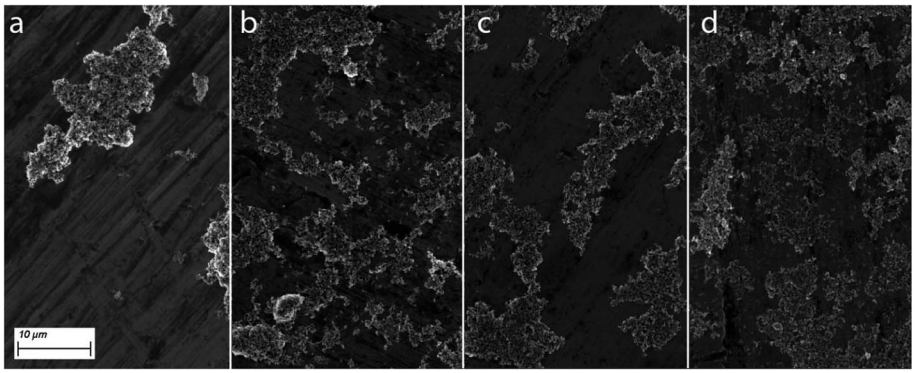

Fig. 2 Scanning electron microscopy images of soot particles with different surface chemistry and aggregate sizes for (a) pristine soot, (b) pristine soot with NOM, (c) NO_2-transformed soot, and (d) NO_2-transformed soot with NOM (same magnification of 1.56k for all).

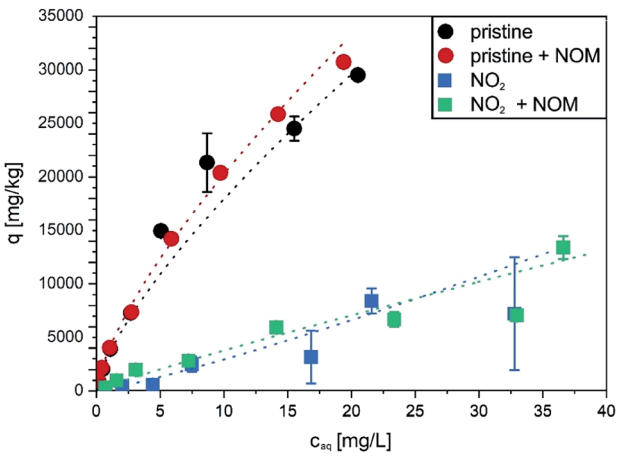

Fig. 3 Sorption of *S*-metolachlor to NO_2-transformed soot was weaker than that to pristine soot. Filled symbols (●, ■) are sorption data, dotted lines are Freundlich sorption isotherm fits.

NOM at concentrations > 20 mg L^{-1}.[40] It should be noted that both the salt (1 mM $CaCl_2$) and the NOM concentration (10 mg L^{-1} DOC) used in this study correspond to concentrations that can be found in natural aquatic environments,[41] and a higher concentration of NOM (*e.g.* 100 mg L^{-1}) may have been able to suppress sorption to soot surfaces *via* competition for sorption sites.[40]

A recently published sorbate-activity-dependent polyparameter linear free-energy relationship (ppLFER) for pristine diesel soot[15] found that the difference in dispersive interactions with the soot *versus* with the water was the dominant factor encouraging adsorption, and H-bonding interactions discouraged this process. We applied the ppLFER proposed by Lu *et al.*[15] using Abraham solute parameters for *S*-metolachlor from the UFZ-LSER database[25] as presented in Table 1 (calculation in Table S1†). The ppLFER predicted that K_D value ranges were in good agreement with the values determined in this study but could not predict the differences observed between pristine soot and NO_2 transformed soot (see Table 4). The discrepancy of K_D values between the ppLFER and this study may partially be explained by differences in the surface chemistry (*e.g.* oxygen containing surface functional groups); however, such data were not reported in the study by Lu *et al.*[15]

Table 3 Freundlich fitting parameters (K_F and n) for *S*-metolachlor with sorption to NO_2-transformed soot being more linear and weaker compared to that to pristine soot

	K_F [mg kg^{-1} (mg $L)^{-n}$]	n [—]	R^2
Pristine	3382 ± 52	0.72 ± 0.01	0.991
Pristine + NOM	3898 ± 70	0.71 ± 0.02	0.991
NO_2	475 ± 46	0.90 ± 0.05	0.956
NO_2 + NOM	198 ± 22	1.17 ± 0.04	0.994

Table 4 The sorption coefficient (K_D) range calculated based on the ppLFER proposed by Lu *et al.*[15] is in the same range as the coefficients derived in this study, but the ppLFER was not able to differentiate between pristine and NO_2-transformed soot. All parameters were calculated at an aqueous concentration of 10 mg L^{-1}

	log K_D from ppLFER	log K_D from Freundlich fit
Pristine	2.86 ± 0.49	3.25 ± 0.12
Pristine + NOM		3.31 ± 0.23
NO_2	2.81 ± 0.49	2.47 ± 0.40
NO_2 + NOM		2.58 ± 0.40

4. Conclusion

Soot is an important naturally occurring CNP that can be found ubiquitously in the environment. During atmospheric transport, soot can be chemically transformed by reactive oxygen species, including NO_2. Our results show that reaction of soot with NO_2 has significant impacts on aggregation and sorption of soot in aquatic environments. Pristine soot is a strong sorbent for *S*-metolachlor, but is likely to rapidly aggregate when introduced directly into surface waters. In contrast, soot that is oxidized by NO_2 shows a decreased sorption for *S*-metolachlor, but exhibits a higher stability against aggregation.

In agreement with findings on other CNPs, soot aggregation decreased in the presence of NOM. NO_2-transformed soot can act as a contaminant vector; however, due to the significantly lower sorption potential for *S*-metolachlor, the expected risk is lower than that for pristine soot or soot stabilized by NOM.

Future research on soot CNP properties should focus on additional transformations and changes in soot properties that can occur in the natural environment. For instance, hetero-aggregation of soot and NO_2-transformed soot with mineral particles remains an underexplored aspect and should be the subject of further investigations.

Conflicts of interest

There are no conflicts to declare.

Acknowledgements

The authors would like to thank Christine Sternkopf (Technical University of Munich) for her help with electron microscopy, as well as Christoph Haisch (Technical University of Munich) and Mehdi Gharasoo (Institute of Groundwater Ecology, Helmholtz Center, Munich) for fruitful discussions. This study was partly funded by the Austrian Science Fund (FWF) [project number P27689-N28] and by the European Research Council (ERC) under the European Union's Seventh Framework Programme (FP7-IDEAS-ERC) [ERC Grant Agreement No. 616861 (MicroDegrade)].

References

1 O. Hoegh-Guldberg, D. Jacob and M. Taylor, *et al.*, Impacts of 1.5 °C global warming on natural and human systems, *Glob Warm 15 °C - IPCC's Spec Assess Rep.*, 2018.
2 H. Wang, Formation of nascent soot and other condensed-phase materials in flames, *Proc. Combust. Inst.*, 2011, **33**(1), 41–67.
3 M. I. Bird, J. G. Wynn, G. Saiz, C. M. Wurster and A. McBeath, The Pyrogenic Carbon Cycle, *Annu. Rev. Earth Planet. Sci.*, 2015, **43**(1), 273–298.
4 G. Sigmund, C. Jiang, T. Hofmann and W. Chen, Environmental transformation of natural and engineered carbon nanoparticles and implications for the fate of organic contaminants, *Environ. Sci.: Nano*, 2018, 2500–2518.
5 J. H. Seinfeld and S. N. Pandis, *Atmospheric Chemistry and Physics: From Air Pollution to Climate Change*, Wiley, 2016.
6 N. Riemer, H. Vogel and B. Vogel, Soot aging time scales in polluted regions during day and night, *Atmos. Chem. Phys.*, 2004, **4**(7), 1885–1893.
7 H. Muckenhuber and H. Grothe, The heterogeneous reaction between soot and NO_2 at elevated temperature, *Carbon*, 2006, **44**(3), 546–559.
8 H. Muckenhuber and H. Grothe, A DRIFTS study of the heterogeneous reaction of NO_2 with carbonaceous materials at elevated temperature, *Carbon*, 2007, **45**(2), 321–329.
9 C. Chen and W. Huang, Aggregation Kinetics of Diesel Soot Nanoparticles in Wet Environments, *Environ. Sci. Technol.*, 2017, **51**(4), 2077–2086.
10 E. J. W. Verwey, N. Laboratorium and D. Waals, Theory of the Stability of Lyophobic Colloids, *J. Phys. Colloid Chem.*, 1947, **51**(3), 631–636.
11 B. Derjaguin and L. Landau, Theory of the stability of strongly charged lyophobic sols and of the adhesion of strongly charged particles in solutions of electrolytes, *Prog. Surf. Sci.*, 1993, **43**(1), 30–59.
12 S. Bhattacharjee, C. Ko and M. Elimelech, DLVO Interaction between Rough Surfaces, *Langmuir*, 1998, **7463**(26), 3365–3375.
13 F. Schwab, L. Camenzuli, K. Knauer, B. Nowack, A. Magrez, L. Sigg, *et al.*, Sorption kinetics and equilibrium of the herbicide diuron to carbon nanotubes or soot in absence and presence of algae, *Environ. Pollut.*, 2014, **192**, 147–153.
14 T. H. Nguyen, I. Sabbah and W. P. Ball, Sorption nonlinearity for organic contaminants with diesel soot: method development and isotherm interpretation, *Environ. Sci. Technol.*, 2004, **38**(13), 3595–3603.
15 Z. Lu, J. K. MacFarlane and P. M. Gschwend, Adsorption of Organic Compounds to Diesel Soot: Frontal Analysis and Polyparameter Linear Free-Energy Relationship, *Environ. Sci. Technol.*, 2016, **50**(1), 285–293.
16 P.-H. Su, D. T. Fu Kuo, Y. Shih and C. Chen, Sorption of organic compounds to two diesel soot black carbons in water evaluated by liquid chromatography and polyparameter linear solvation energy relationship, *Water Res.*, 2018, **144**, 709–718.
17 T. Hüffer, S. Schroth and T. C. Schmidt, Influence of humic acids on sorption of alkanes by carbon nanotubes - implications for the dominant sorption mode, *Chemosphere*, 2015, **119**, 1169–1175.
18 M. Kah, X. Zhang and T. Hofmann, Sorption behavior of carbon nanotubes: changes induced by functionalization, sonication and natural organic matter, *Sci. Total Environ.*, 2014, **497–498**, 133–138, DOI: 10.1016/j.scitotenv.2014.07.112.
19 J. Y. Chen, W. Chen and D. Zhu, Adsorption of nonionic aromatic compounds to single-walled carbon nanotubes: effects of aqueous solution chemistry, *Environ. Sci. Technol.*, 2008, **42**(19), 7225–7230.
20 L. Wang, Y. Huang, A. T. Kan, M. B. Tomson and W. Chen, Enhanced Transport of 2,2′,5,5′-Polychlorinated Biphenyl by Natural Organic Matter (NOM) and Surfactant-Modified Fullerene Nanoparticles (nC_{60}), *Environ. Sci. Technol.*, 2012, **46**(10), 5422–5429.
21 L. Hou, J. D. Fortner, X. Wang, C. Zhang, L. Wang and W. Chen, Complex interplay between formation routes and natural organic matter modification controls capabilities of C_{60} nanoparticles (nC_{60}) to accumulate organic contaminants, *J. Environ. Sci.*, 2017, **51**, 315–323.
22 A. Tsaboula, E. N. Papadakis, Z. Vryzas, A. Kotopoulou, K. Kintzikoglou and E. Papadopoulou-Mourkidou, Environmental and human risk hierarchy of pesticides: a prioritization method, based on monitoring, hazard

assessment and environmental fate, *Environ. Int.*, 2016, **91**, 78–93.

23 National Institutes of Health - Health & Human Services, Hazardous Substances Data Bank (HSDB), 2019, https://toxnet.nlm.nih.gov/cgi-bin/sis/htmlgen?HSDB.

24 S. Endo, P. Grathwohl, S. B. Haderlein and T. C. Schmidt, Effects of Native Organic Material and Water on Sorption Properties of Reference Diesel Soot, *Environ. Sci. Technol.*, 2009, **43**, 3187–3193.

25 N. Ulrich, S. Endo, T. N. Brown, N. Watanabe, G. Bronner and M. H. Abraham, *et al.*, *UFZ-LSER database v 3.2*, Helmholtz Zentrum für Umweltforschung - UFZ, Leipzig, Deutschland, 2017, http://www.ufz.de/lserd.

26 A. Sadezky, H. Muckenhuber, H. Grothe, R. Niessner and U. Pöschl, Raman microspectroscopy of soot and related carbonaceous materials: spectral analysis and structural information, *Carbon*, 2005, **43**(8), 1731–1742.

27 T. Boger, D. Rose, P. Nicolin, N. Gunasekaran and T. Glasson, Oxidation of Soot (Printex® U) in Particulate Filters Operated on Gasoline Engines, *Emiss. Control Sci. Technol.*, 2015, **1**(1), 49–63.

28 Y. Wei, Q. Zhang and J. E. Thompson, The Wetting Behavior of Fresh and Aged Soot Studied through Contact Angle Measurements, *Atmos. Clim. Sci.*, 2017, **07**(01), 11–22.

29 G. Sigmund, T. Hüffer, T. Hofmann and M. Kah, Biochar total surface area and total pore volume determined by N_2 and CO_2 physisorption are strongly influenced by degassing temperature, *Sci. Total Environ.*, 2017, **580**, 770–775.

30 OECD, *Guideline 106 for the testing of chemicals - Adsorption-Desorption Using a Batch Equilibrium Method*, 2000, pp. 1–44.

31 A. Clavier, A. Praetorius and S. Stoll, Determination of nanoparticle heteroaggregation attachment efficiencies and rates in presence of natural organic matter monomers. Monte Carlo modelling, *Sci. Total Environ.*, 2019, **650**, 530–540.

32 R. J. Williams, S. Harrison, V. Keller, J. Kuenen, S. Lofts, A. Praetorius, *et al.*, Models for assessing engineered nanomaterial fate and behaviour in the aquatic environment, *Current Opinion in Environmental Sustainability*, 2019, **36**, 105–115.

33 T. Hüffer, H. Sun, J. D. Kubicki, T. Hofmann and M. Kah, Interactions between aromatic hydrocarbons and functionalized C_{60} fullerenes – insights from experimental data and molecular modelling, *Environ. Sci.: Nano*, 2017, **4**(5), 1045–1053.

34 R. W. Coughlin and F. S. Ezra, Role of Surface Acidity in the Adsorption of Organic Pollutants on the Surface of Carbon, *Environ. Sci. Technol.*, 1968, **2**(4), 291–297.

35 T. J. Bandosz, J. Jagiełło and J. A. Schwarz, Effect of Surface Chemical Groups on Energetic Heterogeneity of Activated Carbons, *Langmuir*, 1993, **9**(10), 2518–2522.

36 H. H. Cho, B. A. Smith, J. D. Wnuk, D. H. Fairbrother and W. P. Ball, Influence of surface oxides on the adsorption of naphthalene onto multiwalled carbon nanotubes, *Environ. Sci. Technol.*, 2008, **42**(8), 2899–2905.

37 K. Yang and B. Xing, Adsorption of organic compounds by carbon nanomaterials in aqueous phase: Polanyi theory and its application, *Chem. Rev.*, 2010, **110**(10), 5989–6008.

38 S. E. Hale, H. P. H. Arp, D. Kupryianchyk and G. Cornelissen, A synthesis of parameters related to the binding of neutral organic compounds to charcoal, *Chemosphere*, 2016, **144**, 65–74.

39 M. Kah, H. Sun, G. Sigmund, T. Hüffer and T. Hofmann, Pyrolysis of waste materials: characterization and prediction of sorption potential across a wide range of mineral contents and pyrolysis temperatures, *Bioresour. Technol.*, 2016, **214**, 225–233.

40 X. Zhang, M. Kah, M. T. O. Jonker and T. Hofmann, Dispersion state and humic acids concentration-dependent sorption of pyrene to carbon nanotubes, *Environ. Sci. Technol.*, 2012, **46**(13), 7166–7173.

41 R. Salminen, M. J. Batista, M. Bidovec, A. Demetriades, B. De Vivo and W. De Vos, *et al.*, *Geochemical Atlas of Europe. Part 1: Background Information, Methodology and Maps - Statistical data of analytical results*, 2005, p. 526.